Supporting information

"Metallo-ROS" in Alzheimer's Disease:

Metal-Centered Oxidation of Neurotransmitters by Cu^{II}-β-Amyloid Provides an Alternative Perspective for the Neuropathology of Alzheimer's Disease

Giordano F. Z. da Silva and Li-June Ming*

Department of Chemistry and Institute for Biomolecular Science

University of South Florida

4202 Fowler Avenue, CHE205

Tampa, FL 33620, USA

E-mail: ming@shell.cas.usf.edu

Table S1

Figures S1–S6

Table S1. Kinetic parameters for the oxidation of catecholamines to *o*-quinone by $A\beta_{1-20}$, except those indicated.

Substrate	k_{cat} (10^{-3} s^{-1})	K' (mM)[a]	k_{cat}/K' ($M^{-1}s^{-1}$)	k_{rel}[b]	k_{cat} (10^{-3} s^{-1}) sat. H_2O_2	k_{cat}/K' ($M^{-1}s^{-1}$)[c] sat. H_2O_2	k'_{rel}[d] sat. H_2O_2
Catechol[e]	154	0.35	440	3.25×10^5	531	1,510	2.24×10^5
(by $A\beta_{1-16}$)	280	0.31	900	5.92×10^5	1,150	1,690	7.64×10^5
(by $A\beta_{1-40}$)[f]	0.87	0.19	4.6	1,850	11.2	28	1.96×10^4
dopamine	11.6	0.90	13	1,320	99	190	5,530
(by $A\beta_{1-16}$)	28	0.31	90	3,180	230	340	1.27×10^4
(by $A\beta_{1-40}$)[f]	0.75	0.27	2.8	85	5.61	11	312
(±) Epinephrine	3.1	0.60	5.2	2,420	24	34	9,420
(–) Epinephrine	2.9	0.61	4.8	2,270	22	54	8,630
(–) Norepinephrine	2.7	0.52	5.2	1,330	17	32	6,940
(+) Norepinephrine	2.8	0.57	4.9	1,380	18	39	7,350
(–) Dopa	1.1	0.34	3.2	333	9.11	27	1,360
(+) Dopa	1.2	0.32	3.8	364	9.03	28	1,350
Phenol[e]	3.9	1.23	3.2	8.67×10^4	213	170	4.16×10^6
(by $A\beta_{1-16}$)	6.4	0.59	11	1.41×10^5	340	58	6.64×10^6

(by $A\beta_{1-40}$)[f]	0.44	1.25	0.35	9.54×10^3	1.43	1.14	2.79×10^4
5-hydroxy-Trp	6.4	0.45	14	8.25×10^3	43.9	97.5	5.64×10^4
serotonin	6.7	1.47	4.5	7.75×10^3	30.4	67.6	3.28×10^4
(by $A\beta_{1-16}$)	26	0.63	41	3.03×10^4	250	380	2.69×10^5
(by $A\beta_{1-40}$)[f]	0.28	0.33	0.84	324	7.8	24.4	8.41×10^3

[a] Intrinsic dissociation constant for the CuAβ-S complex. [b] The background self-oxidation rate constant k_o is calculated based on the MBTH detection of *o*-quinone formation in the absence of CuAβ at 25 °C in 100.0 mM HEPES pH 7.0 under aerobic conditions, wherein the k_o are 4.74×10^{-7},[e] 8.8×10^{-6}, 1.3×10^{-6}, 2.4×10^{-6}, 3.3×10^{-6}, 4.6×10^{-8},[e] 7.78×10^{-7}, and 8.59×10^{-7} s^{-1}, respectively, in the absence of H_2O_2 for catechol, dopamine, (+/–)epinephrine, (–)norepinephrine, L-DOPA, phenol, 5-hydroxy-Trp, and serotonin. [c] *K*' here is the apparent dissociation constant for the (H_2O_2/CuAβ)-S complex. [d] The background rates for the oxidation of catechol, dopamine, epinephrine, norepinephrine, DOPA, phenol, 5-hydroxy-Trp, and serotonin in the presence of 50 mM H_2O_2 are 2.37×10^{-6}, 1.8×10^{-5}, 2.5×10^{-6}, 2.0×10^{-6}, 3.3×10^{-6}, 5.12×10^{-8}, 8.89×10^{-7}, and 9.28×10^{-7} (50 mM), respectively, in 100 mM HEPES at 25 °C and pH 7.0. [e] G.F.Z. da Silva, W.M. Tay, L.-J. Ming, *J. Biol. Chem.* **2005**, *280*, 16601-16609; G.F.Z. da Silva, L.-J. Ming, *Angew. Chem. Int. Ed.* **2005**, *44*, 5501-5504. [f] Kinetic parameters were obtained from the fittings to the Hill equation

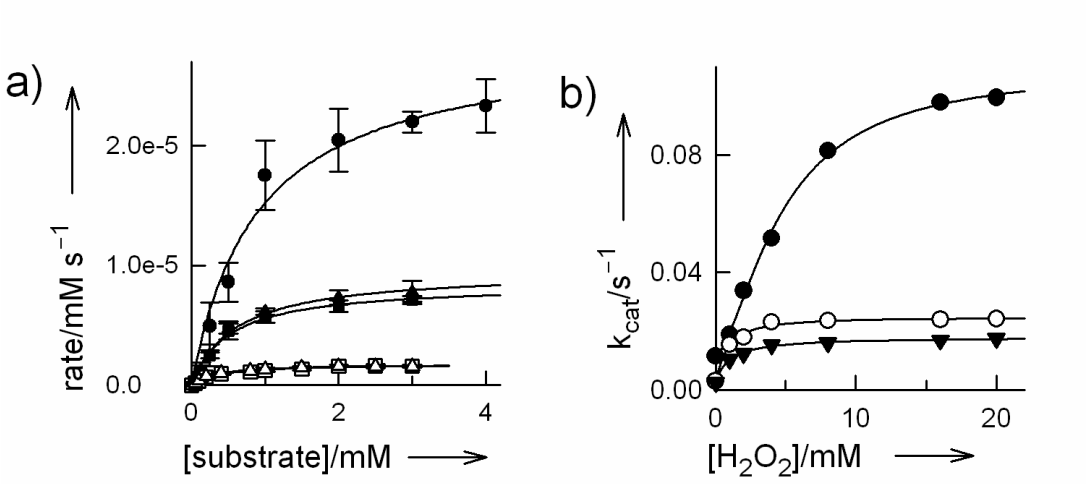

Figure S1. a) Oxidation of the catecholamines dopamine (●), (+/–)epinephrine (▲), (–)norepinephrine (■), L-DOPA (○), and D-DOPA (□) by 2.5 μM CuA$\beta_{1\text{-}20}$ in the absence of H_2O_2. The solid traces are the best fit to an enzyme-like pre-equilibrium kinetics. b) The dependence of the first-order rate constant on [H_2O_2] toward the oxidation of dopamine (●), (+/–)epinephrine (○), and (–) norepinephrine (▼).

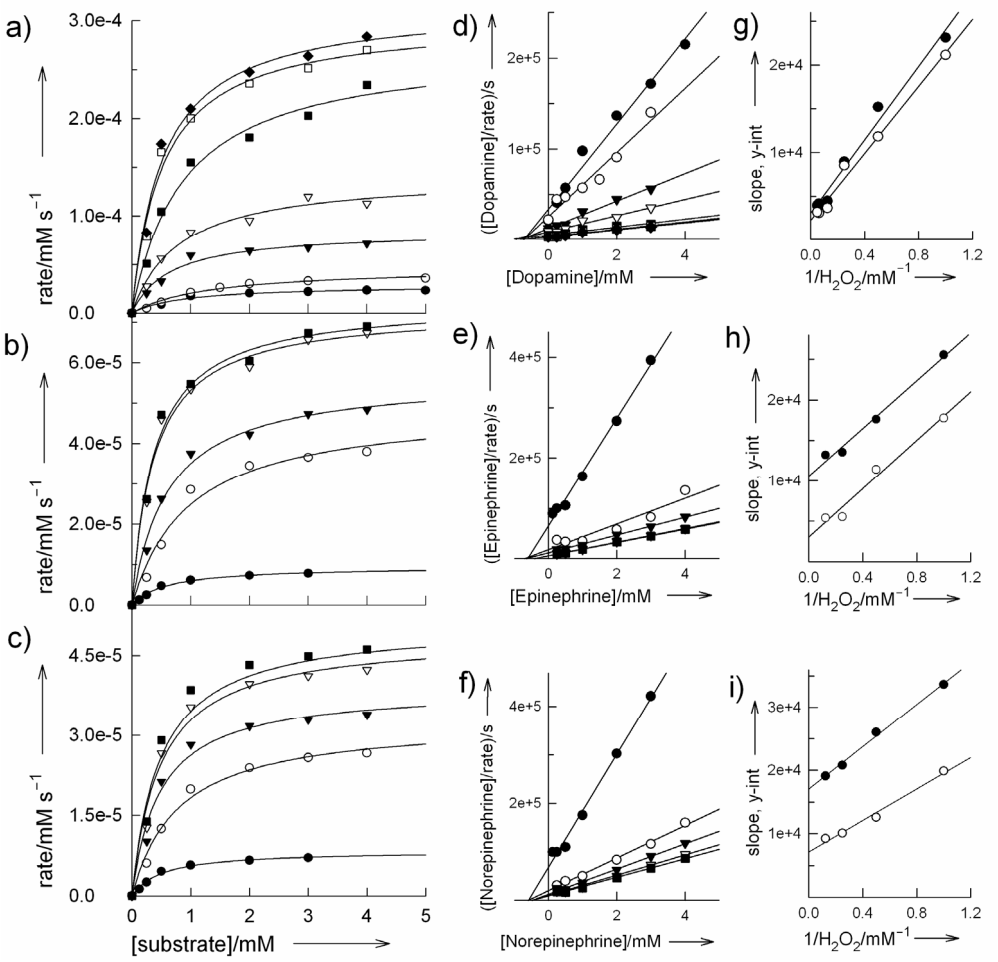

Figure S2. Oxidation of dopamine (a), (+/–)epinephrine (b), and (–)norepinephrine (c) catalyzed by 3.15 μM CuA$\beta_{1\text{-}20}$ in the presence of H_2O_2 (from bottom, 0, 1.0, 2.0, 4.0, 8.0, 16.0, and 20.0 mM). (d–f) Hanes plot analysis of catecholamine oxidation in the presence of H_2O_2 (from plots a–c, respectively). The lines are the best fits to a bi-substrate mechanism. (g–i) Secondary plots of the Hanes plots from d–f which reveal apparent K_S and intrinsic K_{Si} dissociation constants (cf. Fig. 3), by plotting of the slope (•) and y-intercept (o) from plots d–f as a function of 1/[H_2O_2].

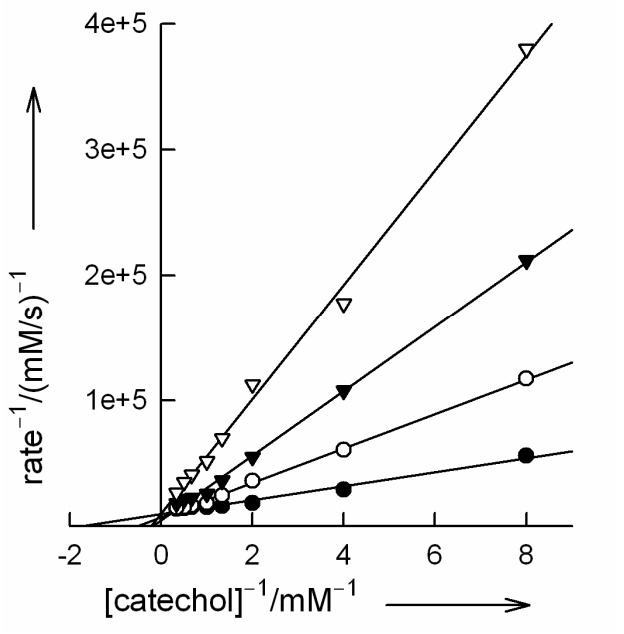

Figure S3. Phosphate inhibition toward catechol oxidation by CuAβ_{1-20} in 100 mM HEPES at pH 7.0. Phosphate concentrations are 0, 10, 20, and 40 mM (from bottom).

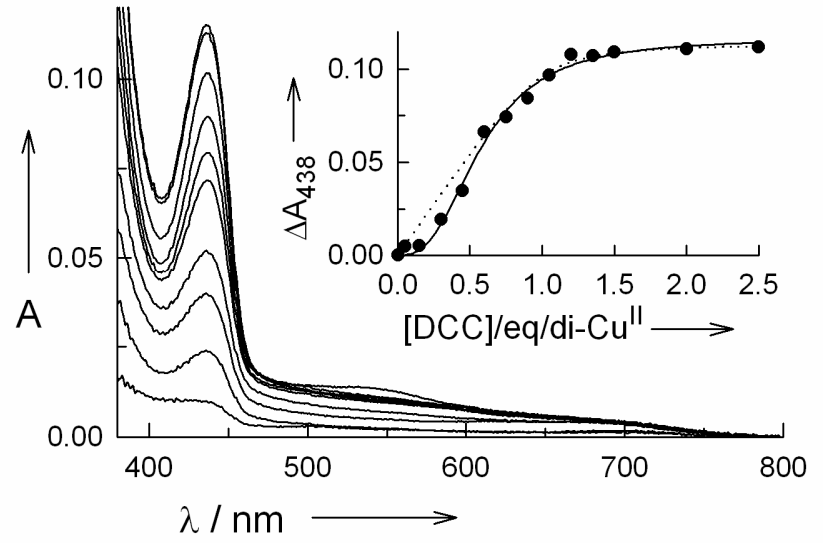

Figure S4. a) Optical titration of 4,5-dichlorocatechol (DCC) into 0.05 mM CuAβ_{1-40}. Inset shows change of intensity at 438 nm upon DCC binding to a di-Cu^{II} center. The dotted trace is the fitting to a simple DCC + diCu $\rightleftharpoons$ DCC-diCu equilibrium, whereas the solid trace is the fitting to consider cooperativity. Both were in 100.0 mM HEPES at pH 7.0.

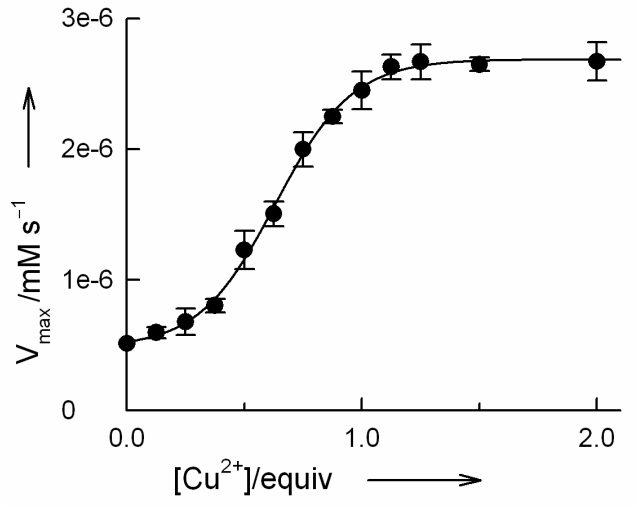

Figure S5. Activity titration of Cu^{II} into 2.5 micro-M $A\beta_{1-40}$ under saturating conditions of catechol.

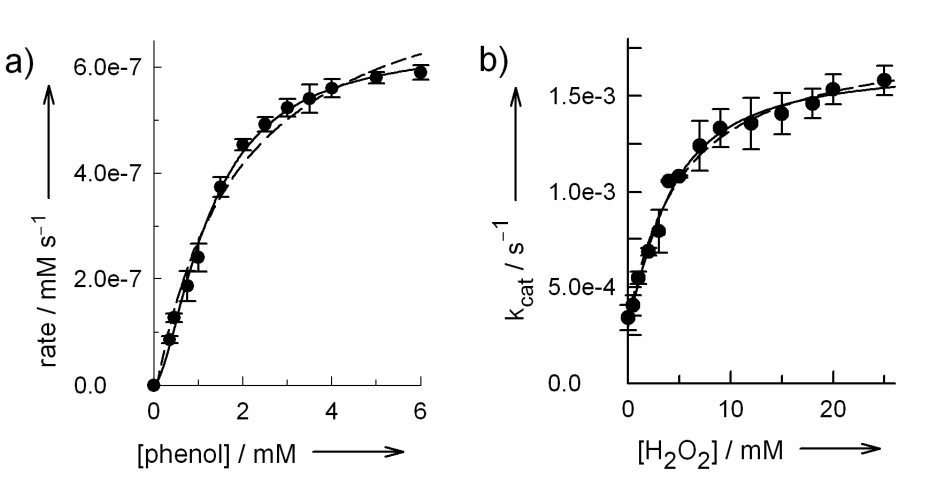

Figure S6. (a) Saturation profile of phenol oxidation by 1.47 μM $CuA\beta_{1-40}$ in 100.0 mM HEPES at pH 7.0 and 25 °C. Dashed line is the fitting to a pre-equilibrium kinetics while the solid line is the fitting to the Hill equation (k_{cat} = 4.39 × 10^{-4}, K_m = 1.25 mM, k_{cat}/ K_m = 0.35 $M^{-1}s^{-1}$, θ = 1.60). (b) The effect of H_2O_2 on the first order rate constant k_{cat}. Cooperativity is not very apparent in this case, showing θ = 1.33.